Development of feedback control system of wall turbulence using MEMS devices

Tsuyoshi YAMAGAMI, Yuji SUZUKI, and Nobuhide Kasagi

Department of Mechanical Engineering, The University of Tokyo,

Hongo 7-3-1, Bunkyo-ku, Tokyo 113-8656, Japan

E-mail: yamagami@thtlab.t.u-tokyo.ac.jp

A prototype of feedback control system of wall turbulence using MEMS sensors and actuators is developed. It consists of 18 hot-film wall-shear stress sensors having backside electronic contact, and 16 microfabricated seesaw-type magnetic actuators working at low energy consumption of 43mW. Spanwise spacing of the sensor and the actuator are both 1mm, which enables us to apply the control system to a higher Reynolds number of $Re_\tau \sim 600$ than our previous control system. The seesaw-type actuators are supported with polyimide hinges, and tilt around their axis aligned in the streamwise direction. Their maximum tilt angle is designed to be 12 degree, which corresponds to the tip displacement of 90μm. Analog VLSI controller including bridge amplifier, signal amplifier, linearizer, GA-based controller, and power amplifier is also designed, and its prototype is fabricated. One VLSI chip can drive two sensors and actuators, and all the circuits for one row of sensors and actuators are implemented with a single print circuit board. The present configuration significantly reduce the power consumption and complexity of the sytem if compared with our 3rd-generation system.

1. Introduction

About seventy years ago, Gray[1] studied swimming performance of dolphins. Based on a bold assumption, he estimated the required weight of muscles in a white-bellied dolphin from its maximum swimming speed, and discovered that it was about seven times as large as the dolphin's actual muscle mass. This is known as "Gray's paradox" and it has been suggested that the compliance of the dolphin's skin reduces the skin friction of turbulence. It still remains unverified whether the compliant wall can actually reduce turbulence skin friction, but his study lead to various attempts of turbulence control.

Feedback control of turbulence was also proposed a few decades ago[2], but the development of such a control system using distributed devices was believed to be extremely difficult until microelectro-mechanical systems (MEMS) technologies make us possible to fabricate various micro sensors and actuators[3,4]. Rathnasingham & Breuer[5] made a control system incorporating three sets of a hot-film shear stress sensor, a piezoelectric cantilever beam actuator, and a DSP controller. They reported reduction in turbulent intensities, but number of the devices is insufficient to observe substantial control effect in their system. Tsao et al.[6] developed a sophisticated integrated chip consisting of hot-film shear stress sensors, magnetic flap actuators, and a drive circuit. However, since a total of 22 masks were needed to develop such a complicated device, fabrication yield remained low and the control effect using arrays of their device was not made. Therefore, even in laboratory experiments, no drag reduction was achieved using feedback control systems in previous studies.

Figure 1 show the road map of our feedback control system. The 1st-generation system is an early proto-type (not shown), and has 24 micro hot-film wall shear stress sensors[7] and 4 wall-deformation magnetic actuators. With this prototype, we tried to identify issues for developing a control system that can be applied

to physical experiments. We obtain 6% reduction of the wall shear stress fluctuations in a turbulent air channel flow with the aid of GA-based optimal control scheme[8]. We also found that the time lag of the control loop is an important factor for effective control system.

The 2nd-generation system is built in order to realize drag reduction in a laboratory experiment. It has four sensor rows and three actuators rows in between. Each sensor row has 48 micro wall-shear stress sensors with 1mm spacing, and each actuator row has 16 wall-deformation actuators with 3mm spacing. A fast digital signal processor (DSP) system having 224 analog input and 96 output channels is used as the controller. The processing time in the DSP is within 0.1ms, and the repetition frequency of the control loop is 5kHz. We have obtained about 7% drag reduction in a turbulent air channel flow for the first time as described in Suzuki et al.[9].

In the 3rd-generation system, we extend the control area by using 8 rows of sensors and 7 rows of actuators. It consists of 288 sensors and 84 actuators. The hot-film wall shear stress sensor is redesigned based on detailed thermal analysis in order to improve its frequency response[10]. A novel feed-through technique is also employed to realize backside electronic contact. The actuator is also redesigned to reduce power consumption and to minimize magnetic cross talk between neighboring actuators[11]. Due to the larger control area, we expect that the 3rd generation system offers larger drag reduction than the 2nd generation.

Although both 2nd- and 3rd-generation systems are for demonstrating drag reduction in our laboratory experiments, the dimensions of magnetic actuators are somewhat large, and they need very large electric energy. Moreover, external circuits for sensors and actuators are bulky, and electrical connection between the components needs hundreds of cables, which makes even laboratory experiments very troublesome.

The final goal of the present study is to develop our 4th-generation system, which is an integrated system using MEMS sensors, actuators, and analog VLSI controllers. Although it is still not straightforward to apply this system to real applications, our challenge is to build a robust MEMS-based control system using state-of-the-art microfabrication technologies.

2. Design of 4th generation system

The schematic view of the 4th generation system presently designed is shown in Fig. 2. It consists of the wall shear stress sensor arrays having backside electric contact[11], seesaw-type magnetic actuator arrays, and analog VLSI controllers. The VLSI controller is designed to drive sensors, signal processors and actuator, and all the components can be connected with a few flat cables, which makes handling of the control system very easy. In principle, connections to external DSPs are not necessary except for optimizing the control parameters using the GA-based scheme; once the control parameters are obtained, the system can be operated by itself.

In this paper, we report the detailed design of the sensor, actuator, and VLSI controller.

2.1 Sensor

The hot-film wall shear stress sensor used in the 4th-generation system is the same as that developed for the 3rd generation (Fig. 3a)[11]. Its spanwise spacing is 1mm, and 18 sensors are aligned in the spanwise direction. A platinum hot-film is deposited on a SiN_X diaphragm ($400 \times 250\mu m^2$) of 1 µm in thickness, and a 200 µm-deep air cavity is formed underneath. Electronic connection is made backside of the chip using solder bond with a flexible print circuit board. .Figure 2b shows the power spectra of the wall shear fluctuations measured in a fully-developed turbulent channel flow. At $Re_\tau = 650$, the present measurement data is in good accordance with the DNS data[12]. The cut-off frequency, where the power of the measurement data is half of the DNS data, is 500Hz, and is sufficiently high under the present experimental condition.

2.2 Actuator

Micro actuators employed in turbulence control must have small dimensions, high operating frequency, large deformation in the wall-normal direction, high durability in harsh operating environment, and low energy consumption. Micro actuators most commonly used are electrostatic ones, which need clean operating environment. Moreover, micro actuators manufactured by MEMS technology have essentially two-dimensional planar structures, so that it is not straightforward to develop actuators having large out-of-plane deformation.

Miniature wall-deformation actuators used in our previous systems have larger spanwise spacing than sensors, which defines the upper limit of the Reynolds number in our control experiment at around $Re_\tau = 300$. Moreover, their maximum power consumption is as large as 5W due to the silicone membrane structure having somewhat large stiffness, so that discrete power amplifiers should be employed. Therefore, development of MEMS actuators operating at low energy consumption is required.

Up to now, various MEMS actuators such as magnetic flap actuators[13], synthetic jet actuators using piezoelectric device[14], wall-deformation pneumatic actuators[15] are developed for flow control. Pimpin et al.[16] also developed micro electrostrictive wall-deformation microactuator having a out-of-plane deformation more than ten times larger that of piezoelectric devices. These actuators should introduce large control effect into the flow, but none of them satisfy all our requirements. Therefore, we design MEMS magnetic actuators having power consumption on the order of 10mW, which can be driven by the analog VLSI as described later.

Endo et al.[17] found in their DNS study that the wall-normal velocity induced by a pair of wall deformation actuators aligned side-by-side is effective in controlling wall turbulence. Yoshino et al.[18] developed a seesaw-type magnetic actuator having polymer permanent magnet on both ends of the seesaw. Generally speaking, magnetic force is decreased rapidly with increasing distance between coil and magnet, but it is not the case for the seesaw configuration, where the distance at either end becomes closer. Bernstein et al.[19] develop a two-axis magnetic mirror using quadrupole coil on the seesaw structure. They realize strong tangential magnetic field by using array of permanent magnet, and obtain large tilt angle of 10 degree with 1mW energy consumption. In the present study, we adopt magnetic actuator with the seesaw structure.

Figure 4a shows the structure of seesaw-type magnetic actuator designed in the present study. The actuator is composed of an elongated Si flap suspended by a pair of polyimide hinge. The dimensions of the Si flap are respectively 7mm and 1mm in the streamwise and spanwise directions. Copper coil is formed on the backside of the flap, and the flap tilts around the streamwise axis by the magnetic force between the coil and an array of permanent magnet underneath. The width and the length of the polyimide hinges are respectively chosen as 100μm and 300μm. The thickness of the Si flap and the hinge is 300 μm and 15 μm, respectively.

Figure 4b depicts the cross section of the actuator. The cross section and the turn of the coil are respectively chosen as $10 \times 10 (\mu m)^2$ and 10, by considering the maximum current driven by the analog VLSI. The maximum tilt angle is designed to be 12.5 degree, which corresponds to 90μm tip displacement, at 43 mW (1.7 V, 25 mA) energy consumption. The resonant frequency is expected to be about 500Hz.

Figure 5a shows the seesaw-type actuator array. One actuator array has 16 flaps aligned in the spanwise direction. Figure 5b shows a magnified view of the polyimide hinge and the Cu coil from the backside. Evaluation of the static and dynamic characteristics of the actuator is presently in progress.

2.3 Analog VLSI Controller

Park et al.[11] report our basic design of the analog VLSI controller using MICS (Multi User Integrated Chips Service)[20]. They fabricated analog devices separately for bridge amplifier, signal amplifier, power amplifier, etc., and made preliminary evaluation. In MICS, master slice method is used, where users can

easily design analog devices only by determining the metal layer pattern connecting pre-designed transistors, capacitors and resistors. After Park et al.[11], we develop a prototype feedback controller using a similar foundry service (Olympus Corp., SA220) and in order to realize the GA-based feedback control[9,21] with a physical device. In SA220, we have 20 independent blocks. We can use each block as a component described above. All the circuit design was simulated using SPICE, and its response was fully characterized beforehand.

The circuit diagram to drive one sensor and actuator is presented in Fig. 6. The circuit includes one bridge amplifier, one signal amplifier, one low pass filter, one linearizer (two multipliers), three multipliers, one adder, and one power amplifier. The bridge amplifier is a simple Wheatstone bridge circuit to drive a hot-film sensor as a constant temperature anemometer. In order to extract the wall shear stress fluctuation, offset voltage input is applied to the signal amplifier using external DA. The gain of the amplifier is set to be 100 according to the typical voltage fluctuation of the sensor output (about 20 mV). Low-pass filter is designed to cut off the signal noise over 2 kHz.

Linearizer using two multipliers is used to compensate the nonlinear response of the sensor. The linear combination used in our GA-based control is realized using three multipliers and one adder. The linearized sensor signal, which corresponds to the wall shear stress fluctuations, is multiplied by weight factor with the multiplier, and summed up with the adder. The three weighting factors are also given by external DAs. Finally, the signal output is amplified with the power amplifier.

The bare VLSI chip fabricated is shown in Fig. 7. The prototype integrated system has 18 sensors and 16 actuators per row, so that a circuit board having 9 VLSI chips are designed and fabricated with a four-layered $200x100(mm)^2$ print circuit board. All the connection is made by using four flat cables, which significantly simplify the manipulation of the control system. The total power consumption is also reduced at least by one order of magnitude if compared with that of the 3rd generation system. The present VLSI has only 20 blocks within a relatively large ceramic package in order to monitor each circuit from the outside. Moreover, the current VLSI controller does not have function to trim each circuit, and thus has to have external analog inputs for adjusting the offset voltage of the devices. However, once the present design is found to be effective, more sophisticated mixed VLSI, which can make the whole the circuits even smaller, can be developed using custom design.

2.4 System configuration to realize turbulence control

Figure 8 shows the configuration of the integrated system with one sensor and control array. After Suzuki et al.[9], driving voltage of the actuator is determined with a GA-based optimal control, and defined by a linear summation of the wall shear stress fluctuations at adjacent three upstream sensors. The sensor output signals are connected to neighboring two VLSI controllers and shared by the GA controllers. The same set of weighting factors are employed for all the circuits, and are given by DAs in DSP. Following the evaluation of sensors, actuators and VLSI controllers, the whole system is integrated and examined in the turbulent channel.

3. Conclusions

The prototype of integrated feedback control system is developed by using MEMS sensors having backside electronic constant, seesaw-type magnetic actuators, and analog VLSI controllers, which significantly reduce the power consumption and complexity if compared with our 3rd-generation system. The analog VLSI controller enables us to employ the GA-based optimal control very efficiently.

References

[1] Gray, J., J. Exp. Biology, Vol. 13, (1936), pp. 192.

[2] Wilkinson, S. P., in Prog. Astronautics and Aeronautics: Viscous Drag Reduction in Boundary Layers, Bushnell, D. M., and Hefner, J. N., eds., Vol. 123, (1990), pp. 479-509, AIAA.

[3] Udell, K. S., Pisano, A. P., Howe, R. T., Muller, R. S., and White, R. M., Exp. Therm. Fluid Sci., Vol. 3, (1990), pp. 52-59.

[4] Ho, C.-M., and Tai, Y.-C., ASME J. Fluids Eng. Vol. 118, (1996), pp. 437-447.

[5] Rathnasingham, R., and Breuer, K., Phys. Fluids, Vol. 9, (1997), pp. L1867-L1869.

[6] Tsao, T., Jiang, F., Miller, R. A., Tai, Y. C., Gupta, B., Goodman, R., Tung, S., and Ho, C. -M., Tech. Digest Int. Conf. on Solid-State Sensors and Actuators (Transducers '97), (1997), Chicago, pp. 315-317.

[7] Yoshino. T, Suzuki, Y., and N. Kasagi, Proc. 2nd Int. Symp. Turbulence and Shear Flow Phenomena, (2001), Stockholm, Vol. II, pp. 17-22.

[8] Suzuki, Y., Yoshino, T., and Kasagi, N., Proc. 4th Symp. Smart Control of Turbulence, (2003), pp. 115-122.

[9] Suzuki, Y., Yoshino, T., Yamagami, T., and Kasagi, N., Proc. 6th Symp. Smart Control of Turbulence, (2005), to be presented.

[10] Yoshino, T., Suzuki, Y., Kasagi, N., and Kamiunten, S., Proc. 16th IEEE Int. Conf. MEMS, Kyoto, (2003), pp. 193-196.

[11] Park, J., Yoshino, T., Suzuki, Y., and Kasagi, N., Proc. 5th Symp. on Smart Control of Turbulence, (2004), pp. 111-117.

[12] Iwamoto, K., Suzuki, Y., and Kasagi, N., Int. J. Heat & Fluid Flow, Vol. 23, (2002), pp. 678-689.

[13] Liu, C., Tsao, T., Lee, G. B., Leu, J., Yi, Y., Tai, Y.-C., and Ho, C.-M., Sensors Actuators A:, Vol. 78, (1999), pp.190-197.

[14] Glezer, A., and Amitay, M., Annu. Rev. Fluid Mech., Vol. 34, 2002, pp. 503-529.

[15] Grosjean, C., Lee, G., Hong, W., Tai, Y.-C., and Ho, C.-M., Proc. 11th IEEE Int. Conf. MEMS, Heidelberg, (1998), pp. 137-142.

[16] Pimpin, A., Suzuki, Y., and Kasagi, N., Proc. 17th IEEE Int. Conf. MEMS, (2004), Maastricht, pp. 478-481.

[17] Endo, T., Kasagi, N., and Suzuki, Y., Int. J. Heat & Fluid Flow, Vol. 21, (2000), pp. 568-575.

[18] Yoshino, T., Tsuda, M., Suzuki, Y., and Kasagi, N., Proc. 3rd Symp. on Smart Control of Turbulence, (2002), pp. 111-117.

[19] Bernstein, J., Taylor, W. P., Brazzle, J., Kirkos, G., Odhner, J., Pareek, A., and Zai, M., Proc. 16th IEEE Int. Conf. MEMS, (2003), Kyoto, pp. 275-278.

[20] Maenaka, K., Asada, K., Okamoto, K., Fujita, T., and Maeda, M., Tech. Digest 16th Sensor Symp., (1998), pp. 227-230.

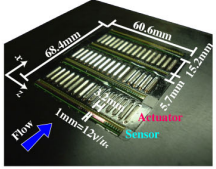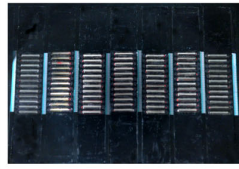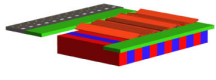[21] Morimoto, S., Iwamoto, K., Suzuki, Y., and Kasagi, N., Bull. Am. Phys. Soc., Vol. 46, (2001), p. 185.

	2nd Generation	3rd Generation	4th Generation
Sensor	Slow Response Frontside Contact	Fast Response Backside Contact	
Actuator	Miniature Prototype	Miniature Improved	MEMS
Controller	Fast DSP (~0.1ms)		AnalogVLSI

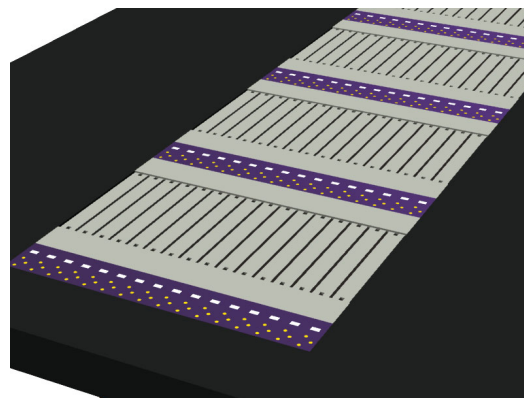Figure 1 Road map of feedback control system for wall turbulence.

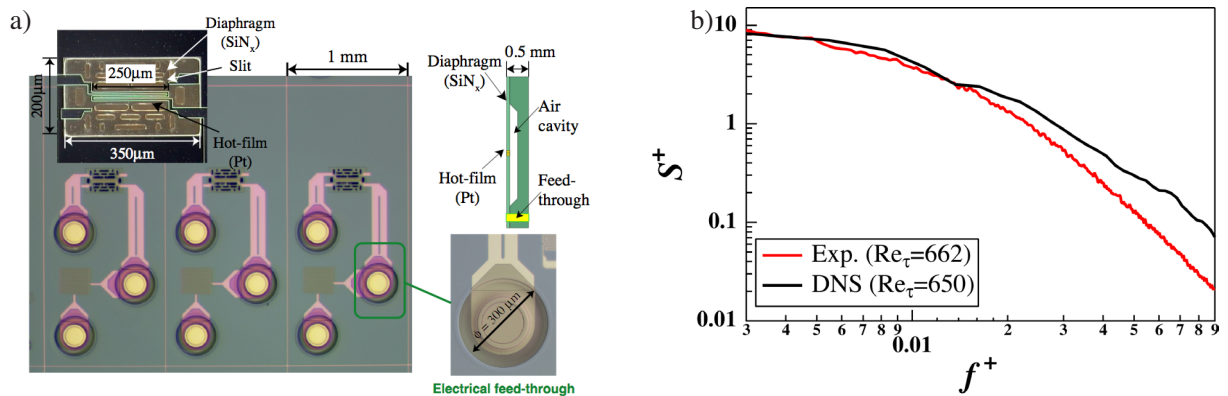Figure 2 Schematic of the 4th-generation feedback control system.

Figure 3 Hot-film wall shear stress sensor with backside contract.　a) Magnified view b) Spectra of the wall shear stress fluctuations measured in a fully-developed turbulent channel flow at Re_τ=662.
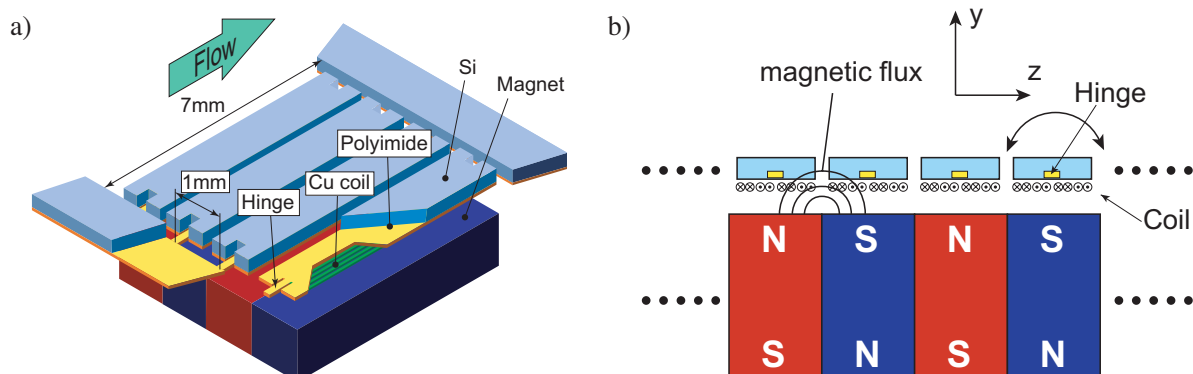
Figure 4 Schematic of seesaw-type magnetic actuator. a)Bird's-eye view, b)Cross sectional view.
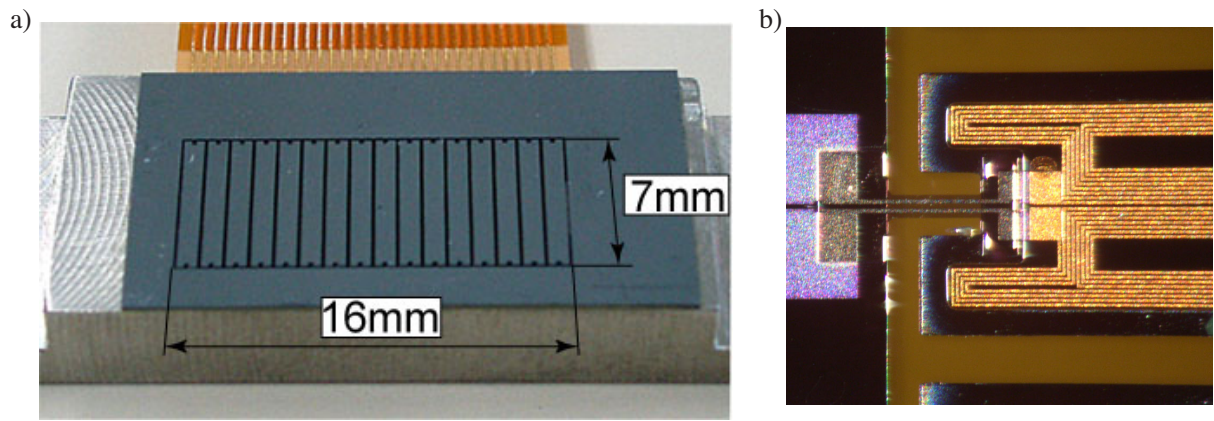
Figure 5 Photograph of seesaw-type magnetic actuators. a) Actuator array assembled, b) Magnified view of a hinge and Cu coil.
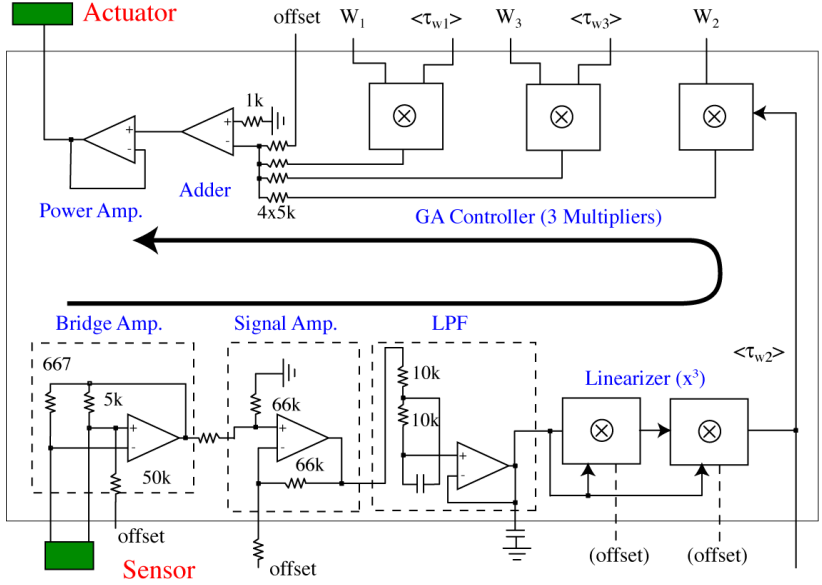

Figure 6 Diagram of the internal circuits of the analog VLSI. Each circuit driving one sensor and actuator has 10 internal blocks. Quantities τ_{w1} and τ_{w3} are the adjacent sensor outputs, and control parameters $W_1 \sim W_3$ are given by DA converters of DSP.
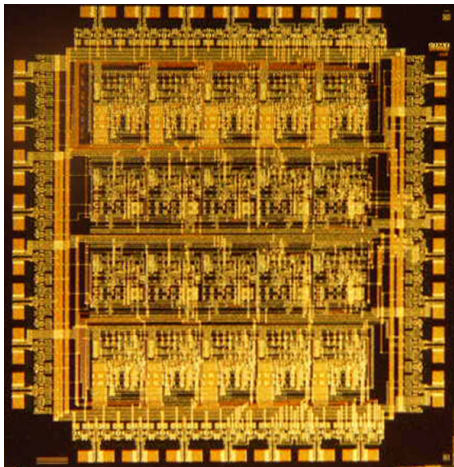

Figure 7 Top view of analog VLSI chip. The dimension is 4.7 x 4.6 mm. Each VLSI contains 2 identical control circuits.
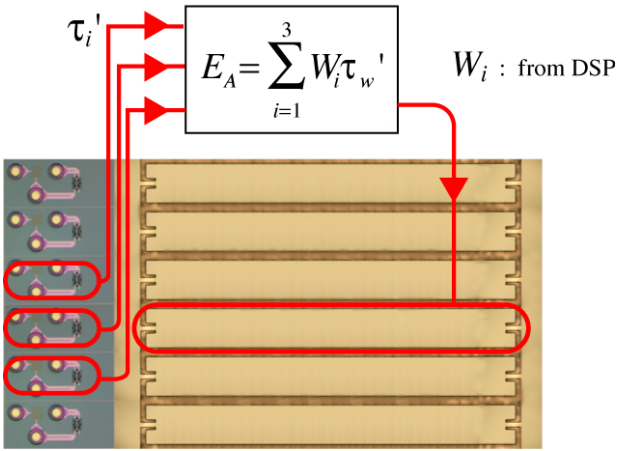

Figure 8 Configuration of the control system integrated with the sensor and actuator arrays.